JoVE: Science Education

Flow Visualization of Flow Past a Bluff Body Using Hydrogen Bubbles

--Manuscript Draft--

Manuscript Number:	10435
Full Title:	Flow Visualization of Flow Past a Bluff Body Using Hydrogen Bubbles
Article Type:	Manuscript
Section/Category:	Manuscript Submission
Corresponding Author:	Ricardo Mejia-Alvarez UNITED STATES
Corresponding Author Secondary Information:	
Corresponding Author's Institution:	
Corresponding Author's Secondary Institution:	
First Author:	Ricardo Mejia-Alvarez
First Author Secondary Information:	
Order of Authors:	Ricardo Mejia-Alvarez
Order of Authors Secondary Information:	

PI Name:

Ricardo Mejia-Alvarez, PhD. Michigan State University

Science Education Title:

Flow Visualization of Flow Past a Bluff Body Using Hydrogen Bubbles

Overview

Owing to the non-linear nature of its governing laws, fluid motion induces complicated flow patterns. Understanding the nature of these patterns has been the subject of intense scrutiny for centuries. ~~Early examples of pattern characterization of fluid flow phenomena for which we still have records, go as early as the XV century when Leonardo Da Vinci produced a set of insightful sketches of what we nowadays consider turbulent flow [1, 2]. Due to their complexity, it is still not possible to predict the emergence and exact behavior of all flow patterns on theoretical grounds alone. On the other hand, while~~Although personal computers and supercomputers are extensively used to deduce fluid flow patterns, their capabilities are still insufficient to determine the exact flow behavior for complex geometries or highly inertial flows (e.g. when momentum dominates over viscous resistance). With this in mind, a multitude of experimental techniques to make flow patterns evident have been developed that can reach flow regimes and geometries inaccessible to theoretical and computational tools.

This demonstration will investigate fluid flow around a bluff body. A bluff body is an object that, due to its shape, causes separated flow over most of its surface. This is in contrast to a streamlined body, like an airfoil, which is aligned in the stream and causes less flow separation. The purpose of this study is to ~~demonstrate the implementation~~use ~~of~~ hydrogen bubbles as a method of ~~of flow visualization~~visualizing flow patterns. The h~~H~~ydrogen bubbles are produced via electrolysis using a DC power source by submerging its electrodes in the water. Hydrogen bubbles are formed in the negative electrode, which needs to be a very fine wire to ensure that the bubbles remain small and track fluid motion more effectively. ~~:~~

This ~~to educe flow patterns. This~~ method is suitable for steady and unsteady laminar flows, and is based on the basic flow lines that describe the nature of the flow around objects. [1-3] ~~:~~

~~Pathline: path that a fluid particle follows as it moves with the flow.~~

~~Streakline: continuous locus of all the fluid particles whose motion originated at the same spatial location.~~

~~Timeline: set of fluid particles that were tagged at the same instant of time while forming a continuous locus.~~

~~Streamline: continuous line that is everywhere tangent to the velocity field at an instant in time.~~

Commented [DN1]: Adding a statement at the start describing the significance of the topic really gets the viewer engaged. It would be great if you could please add a sentence or two explaining why flow visualization of flow past a bluff body is important to a mechanical engineer?

I am also not sure if we should define a bluff body or not? I leave that up to the authors.

Commented [RM2R1]: I addressed these comments at the end of this section

Commented [DN3]: Should we briefly define these different types of flow lines?

Formatted: No bullets or numbering

~~The first three lines are relatively easy to generate experimentally, while streamlines are merely a mathematical concept that in general have to be produced by post-processing an instantaneous capture of the velocity field. While this is always true, the analysis simplifies significantly in steady flows because pathlines, streaklines, and streamlines coincide with each other. Conversely, these lines do not generally coincide with each other in unsteady flows. (streaklines, pathlines, timelines, and streamlines [1]) that describe the nature of the flow around objects. The implementation of this technique is generally simple and requires only low-cost equipment, as opposed to more sophisticated and expensive techniques such as Particle Image Velocimetry [1], Particle Tracking Velocimetry [53,64], and Molecular Tagging Velocimetry [75].~~

~~Hydrogen bubbles are produced via electrolysis using a DC power source by submerging its electrodes in the water. Hydrogen bubbles are formed in the negative electrode, which needs to be a very fine wire to ensure that the bubbles remain small and track fluid motion more effectively.~~

This paper focuses on describing the implementation of the technique, including details about the equipment and its installation. Then, the technique is used to demonstrate the use of two of the basics flow lines ~~(streaklines and timelines)~~ to characterize the flow around a circular cylinder. These flow lines are used to ~~determine flow patterns such as vortex shedding and~~ estimate some important flow parameters like flow velocity and the Reynolds number, and to determine flow patterns ~~such as vortex shedding. This last process is typical in flow past bluff bodies which, as opposed to streamlined bodies, exhibit boundary layer separation over a substantial portion of their surface. This boundary layer separation leads to the formation of vortices behind the body that could eventually detach periodically into the wake. When periodical detachment takes place, the vortices generate alternating areas of low pressure behind the body that could become resonant loads if the shedding frequency coincides with the natural frequency of the body. Avoiding this scenario is of significant importance in designing engineering structures such as smoke stacks and bridge pillars since it could result in catastrophic failure.~~

Principles

~~During the present experiments, we will use flow lines to study external flow around a circular cylinder.~~ In this configuration, we will consider a uniform steady flow of water with velocity U_∞ (dubbed free-stream velocity) approaching a circular cylinder (~~see~~ Figure 1 ~~for reference~~). Depending on flow conditions as characterized by the Reynolds number, this flow might become unstable and give ~~place to a~~rise to vortex-shedding. ~~process commonly known as the "Von Kármàn vortex street" (see Figure 2 for reference).~~Vortex shedding is typical in flow past bluff bodies which, as opposed to streamlined bodies, exhibit boundary layer separation over a substantial portion of their surface. This boundary layer separation leads to the formation of vortices behind the body that could eventually detach periodically into the wake. When periodical detachment takes place, the vortices generate alternating areas of low pressure behind the body that could become resonant loads if the shedding frequency coincides with the natural frequency of the body. ~~Avoiding this scenario is of significant importance in designing engineering structures such as smoke stacks and bridge pillars since it could result in catastrophic failure.~~ Theis vortex

Commented [DN4]: Should we briefly define these different types of flow lines?

Commented [DN5]: Can we please briefly define this?

Commented [DN6]: Can we please briefly define this?

Formatted: Font color: Text 1

Commented [DN8]: Can we please expand on this statement a little bit, maybe by using example values for Reynolds number, and explain what unstable means here?

Commented [DN7]: Can we please briefly define this?

Commented [RM9R8]: I added some related information in subsequent paragraphs

shedding process is called the ~~process commonly known as the~~ "Von Kármàn vortex street" ~~(see~~ Figure 2 ~~for reference)~~ ~~is often observed~~. This ~~)a~~ repeating pattern of swirling vortices is caused by unsteady flow separation around the bluff body and occurs at certain ranges of Reynolds number. Avoiding this scenario is of significant importance in designing engineering structures such as smoke stacks and bridge pillars since it could result in catastrophic failure.

Commented [DN10]: Can we please briefly define this?

The Reynolds number is a dimensionless parameter defined as the ratio of inertial forces to viscous forces:

$$\mathrm{Re} = U_\infty D/\nu \quad (1)$$

Where ν is the kinematic viscosity of the fluid, V a characteristic velocity (U_∞ in the present case), and D the cylinder diameter. The Reynolds number is arguably the most important parameter in the characterization of fluid flow and will be used throughout the present experiment as the metric for the emergence of the Von Kármàn vortex street. In particular, when the Reynolds number is around 5, the flow exhibits two stable counter-rotating vortices behind the cylinder. As the Reynolds number increases, these two vortices elongate in the direction of the flow. When the Reynolds number reaches a value of approximately 37, the wake becomes unstable and begins to oscillate sinusoidally as a result of an imbalance between pressure and momentum. A further increase in Reynolds number up to 47 causes the two counter-rotating vortices to detach from the cylinder in an alternating sequence that follows the sinusoidal wake oscillation [~~8~~4,5,6~~, 9, 10~~].

The frequency with which vortices are shed off the cylinder is not constant; it varies with the value of the Reynolds number. Shedding frequency is characterized by the~~. The~~ Strouhal number, which is the other~~is another~~ dimensionless parameter of relevance in ~~that is relevant to~~ this particular fluid flow configuration ~~because it characterizes the frequency of vortex shedding~~:

$$\mathrm{St} = fD/U_\infty \quad (2)$$

Here, f is the vortex shedding frequency and the length and velocity scales are the same as for the Reynolds number. Vortex shedding frequency can then be characterized by the Strouhal number as a linear function of the inverse square root of the Reynolds number [7~~11~~]:

$$\mathrm{St} = \mathrm{St}^* + \frac{m}{\sqrt{\mathrm{Re}}} \quad (3)$$

This function is not always monotonic, it exhibits further transitions as a result of secondary instabilities owed to the non-linearity of fluid flow. As a result, the coefficients St^* and m would change according to the Reynolds number range. Table 1 shows the values of these coefficients for the flow regimes that have been well characterized in the literature [7~~11~~].

During the present experiments, we will use flow lines to study external flow around a circular cylinder. These flow lines are defined as follows:

- Pathline: path that a fluid particle follows as it moves with the flow.
- Streakline: continuous locus of all the fluid particles whose motion originated at the same spatial location.
- Timeline: set of fluid particles that were tagged at the same instant of time while forming a continuous locus.
- Streamline: continuous line that is everywhere tangent to the velocity field at an instant in time.

The first three lines are relatively easy to generate experimentally, while streamlines are merely a mathematical concept that in general have to be produced by post-processing an instantaneous capture of the velocity field. While this is always true, the analysis simplifies significantly in steady flows because pathlines, streaklines, and streamlines coincide with each other. Conversely, these lines do not generally coincide with each other in unsteady flows. The implementation of this technique is generally simple and requires only low-cost equipment, as opposed to more sophisticated and expensive techniques such as Particle Image Velocimetry [1], Particle Tracking Velocimetry [5,6,8,9], and Molecular Tagging Velocimetry [7,10].

Procedure

1. To produce a continuous sheet of bubbles:
   1.1. Set the equipment according to the electrical diagram shown in Figure 3.
   1.2. Fix the positive electrode in the water at the downstream end of the test section (see Figure 4 for reference).
   1.3. Fix the negative electrode upstream and near the point of interest to release the bubbles into the stream before the flow reaches the object of study (see Figure 4 for reference). The water completes the circuit between the two electrodes.
   1.4. Turn on the flow facility
   1.5. Set the dial of the frequency controller to position 2. This will establish a flow rate of about 9×10^{-4} m^3/s.
   1.6. Turn on the DC power supply and increase the voltage up to about 25 V, the current will set itself around 190 mA.
   1.7. Set the wave form in the signal generator to Square Wave (symbol: ⊓⊔). This generates a 0 V – 5 V square signal that activates the solid-state relay (closing the circuit) in its high position and opens it in the low position
   1.8. For this particular case, the frequency of the square wave is not important. It just needs to be non-zero.
   1.9. Maximize the DC offset (+5 V) in the signal generator. With this setting, the circuit is always closed and the system generates bubbles continuously.

2. To produce timelines:
   2.1. Turn on the flow facility
   2.2. Set the dial of the frequency controller to position 2. This will establish a flow rate

of about 9×10^{-4} m^3/s.

2.3. Turn on the DC power supply and increase the voltage up to about 25 V, the current will set itself around 190 mA.

2.4. Set the wave form in the signal generator to Square Wave (symbol: ⊓⊔). This generates a 0 V – 5 V square signal that activates the solid-state relay (closing the circuit) in its high position and deactivates it (opening the circuit) in the low position

2.5. Set the DC offset in the signal generator at +1 V.

2.6. Set the frequency of the square wave in the signal generator at 10 Hz.

2.7. Set the symmetry of the square wave slightly negative (-2) to increase the space between timelines while conserving the right frequency.

3. To use flow lines to study Von Kármàn vortex streets:

3.1. Measure the diameter of the rod, D_o, using a caliper. Use S.I. units for this measurement (m).

~~3.1.~~3.2. Fix a cylindrical rod downstream of the negative electrode.

~~3.2.~~3.3. Cast the light of the high-intensity discharge lamp on the layer of hydrogen bubbles. Make sure the light is not directly behind of the line of view to prevent oversaturation of the imaging system

3.4. Align the visualization system with the rod; in a way that only the circular tip is visible in front of the camera.

~~3.3.~~3.5. Add a mark in the visualization window and downstream of the rod to use it as the reference to count vortex-shed cycles per unit time.

4. Data analysis for flow past a circular cylinder:

4.1. Determination of the conversion factor from machine units to real space units:

4.1.1. Measure the width of the shadow cast by the rod on the bubble sheet (see figure 2(A) for reference). Take this measurement right at the rod to avoid distortion with distance. This is the diameter of the rod in machine units, D_i (points or pixels, depending on format)

4.1.2. Use the following equation to determine the conversion factor from machine units to real world units:

$$M = \frac{D_i}{D_o} \qquad (3)(4)$$

Commented [DN11]: It would be great if you could please provide a figure here, so that we understand where this measurement is being made. This will help the scriptwriter when they are converting this manuscript into a script for filming purposes.

Commented [RM12R11]: The figure already exists, it is figure 2a. I added a reference to it here.

4.2. Determination of flow velocity:

4.2.1. Choose a group of undistorted timelines upstream of the bluff body.

4.2.2. Measure the distance between the first and last timeline in machine units, L (points or pixels).

4.2.3. Count the number of timelines in the group, N_{tl}.

4.2.4. Take note of the frequency of the square wave signal as produced by the signal generator, f_{tl}.

4.2.5. Determine the approaching flow velocity from the following equation:

$$U_\infty = \frac{L \cdot f_{tl}}{N_{tl} \cdot M} \quad (4)(5)$$

4.3. Determination of the Reynolds number:

4.3.1. Find the kinematic viscosity of the working fluid (e.g. water $\nu = 1.004 \times 10^{-6}$ m^2/s).

4.3.2. Calculate the Reynolds number using equation (1). For that, considering the diameter of the rod (D_o) measured in step 3.1, ~~Error! Reference source not found.~~4.1.1, the approaching velocity (U_∞) determined with equation (5), and the kinematic viscosity determined in step 4.3.1

4.4. Determination of the Strouhal number: the vortices in the wake of the rod are moving at a different velocity as the timelines in the free stream. Hence, the frequency of vortex shedding needs to be estimated independently.

4.4.1. Define a fixed reference downstream of the rod. This reference could be a fine string attached to the exterior of the tunnel or a digital line added to a video of the flow process.

4.4.2. Count the number of vortex shedding cycles, N_s, crossing the reference during a defined period of time T. A vortex shedding cycle is illustrated in Figure 2(A).

4.4.3. Calculate the shedding frequency from the following equation:

$$f_s = \frac{N_s}{T} \quad (5)(6)$$

4.4.4. Use the results from equations (5) and (6) in equation (2) to calculate the Strouhal number.

Representative Results

Figure 2 shows two representative results of hydrogen bubble visualization of a Von Kármàn vortex street. Figure 2(A) shows an example of a field of streaklines as evidenced by disturbances in the hydrogen bubble sheet. This image is used to extract the diameter of the rod in machine units. Figure 2(B) shows an example of a field of timelines. This image is used to estimate the approaching fluid velocity. The parameters extracted from this particular experiment are summarized in table 2.~~on~~

Since the Reynolds number is 115 for the present example, ~~The~~ the validity of this result can be tested using equation (3) for $47 < \mathrm{Re} < 180$~~a well – established relationship between the Reynolds number and the Strouhal number~~:

$$\mathrm{St} = 0.2684 - \mathrm{St}^* + \frac{1.0356m}{\sqrt{\mathrm{Re}}}, \quad \mathrm{St}^* = 0.2684, \quad m = -1.0356, \quad \text{for } 47 < \mathrm{Re} < 180 \quad (6)(7)$$

Commented [DN13]: If we are using this method to create a reference point, then we should add this step into the protocol above.

Commented [RM14R13]: done

Commented [DN15]: This sentence seems to be incomplete.

Commented [DN16]: Since we are using this as the main formula for results, do you think we should include this relation in principles and explain the variables there?

Commented [RM17R16]: done

~~In the present case~~From which ~~,~~ we obtain:

$$St = 0.172 \qquad (~~7~~8)$$

After comparing this estimation with our experimental result (see table ~~1~~ 2 for reference), we can conclude that our experiment offered a satisfactory result. Figure 5 shows a set of experimental results compared with the predictions of equation (~~6~~7).

Summary

In this study, the usage of hydrogen bubbles was demonstrated to extract qualitative and quantitative information from images of flow around a circular cylinder. The quantitative information extracted from these experiments included the free-stream velocity (U_∞), vortex-shedding frequency (f), Reynolds number (Re), and the Strouhal number (St). In particular, the results for St vs Re exhibited very good agreement with previous studies [3~~1~~16~~6~~].

Due to the slow velocity used in the current experiments, perturbations in the bubble sheet produce a streaky bubble layer. These streaks are basically streaklines. As the hydrogen bubble sheet travels downstream, these streaklines thicken and become more irregular. This is the result of turbulence intensity in the free-stream. The effect is attenuated as the velocity of the tunnel is increased since the bubbles leave the test section before presenting a significant dispersion. Streaklines can also be produced at pre-selected locations by coating the wire while leaving small parts of it exposed to water.

Applications

The current flow behavior is directly applicable to flow past engineering structures such as the pillars of bridges and offshore oil-rigs, wind turbine towers, or power line poles to name a few. And in fact, this behavior is exhibited by bluff bodies with geometries other than cylindrical such as sky scrapers. Given that vortices generate fluid-structure interactions that make structures oscillate, knowing the vortex shedding frequencies at which a given structure will be exposed is critical for its design. In that regard, the engineer has to make sure that the natural frequency of the structure is not such that it will resonate with the vortex shedding frequency, because this effect will inevitably lead to catastrophic failure of the structure. Using appropriate scaling laws [20] and hydrogen bubbles in a water tunnel, an engineer can simulate the interaction of flow with a structure prior to its construction to make sure that its design is safe or to find out if it needs any modifications.

Besides bluff bodies, hydrogen bubble visualization is a very powerful tool to study flow around streamlined bodies such as airfoils or ship hulls. By making use of flow lines generated with this technique, one can determine parameters such as the angle of attack at which stall takes place, or even estimate lift characteristics based on flow velocity. More importantly, the pattern of distortion of fluid lines will help the engineer to optimize its design.

Visualization with hydrogen bubbles is not restricted to external flows like the above mentioned. This method can also be used to observe the flow through open channels or

Commented [DN18]: Is it possible to film a couple of applications at your lab? Perhaps we can show the flow pattern for a different shape object?

Also, will it be possible to film flow across streamlined bodies? That could be one of the applications.

Commented [RM19R18]: Yes, all of this is possible

fully confined flow systems. In the latter case, the walls will need to be transparent to ensure optical access. For example, if one is interested in designing a flow diffuser for sub-sonic flow, hydrogen bubbles can be used to determine geometric and flow conditions for which the diffuser will exhibit flow separation and instability. Based on those observations, the design could be experimentally optimized to ensure its proper functionality.

Materials List

Name	Company	Catalog Number	Comments
Equipment			
DC power supply	Hewlett Packard	E3612A	Input: 120VAC; Output: 0-60VDC, 0-0.5A
Signal generator	Wavetek	19	
Solid-state relay	Magnecraft	W171DIP-7DC	
Water tunnel	ELD	Model 6"	With frequency controller
High-intensity discharge lamp			Tungsten-Halogen
Aluminum rod			Positive electrode
Stainless-steel fork			To hold a 50.8 μm stainless-steel wire as the negative electrode

Figures and tables captions

Figure 1. Flow past a circular cylinder. Schematic of basic configuration. A homogeneous stream with velocity U_∞ approaches a straight cylinder of diameter D whose axis of symmetry is perpendicular to the approaching velocity.

Figure 2. Representative results. (A) continuous sheet of hydrogen bubbles that shows streaklines as a result of upstream disturbances. The shadow cast by the rod is used to determine the conversion from machine to real units. A vortex shedding cycle is also illustrated to help determine shedding frequency appropriately. (B) timelines generated with hydrogen bubbles. Since timeline frequency is well-defined, they can be used to measure flow velocity accurately; counting the timelines enclosed in the red lines will be used for this estimation.

Figure 3. Connections diagram.

Figure 4. Test section. Flow goes from left to right. The negative electrode generates a layer of hydrogen bubbles that are swept away with the flow. The positive electrode is set at the downstream end of the test section to avoid its disturbances.

Figure 5. Experimental results. Comparison of current experimental results against predictions of the relation between the Reynolds number and the Strouhal number for flow past a circular cylinder.

Table 1. Values of the coefficients St^* and m **for different Reynolds number intervals (from [8~~11~~]).**

Table ~~1~~2. Representative results for flow past a circular cylinder.

References

1. Zöllner, F. Leonardo da Vinci 1452-1519: sketches and drawings, Taschen, 2004.
~~1.~~2. White, F. M. Fluid Mechanics, 7th ed., McGraw-Hill, 2009.
~~2.~~3. Adrian, Ronald J., and Jerry Westerweel. Particle Image Velocimetry. Cambridge University Press, 2011.
~~3.~~4. Gerrard, J. H., The wakes of cylindrical bluff bodies at low Reynolds number, Phil. Trans. Roy. Soc. (London) Ser. A, Vol. 288, No. 1354, pp. 351-382 (1978)
~~4.~~5. Coutanceau, M. and Bouard, R., Experimental determination of the viscous flow in the wake of a circular cylinder in uniform translation. Part 1. Steady flow, J. Fluid Mech., Vol. 79, Part 2, pp. 231-256 (1977)
~~5.~~6. Kovásznay, L. S. G., Hot-wire investigation of the wake behind cylinders at low Reynolds numbers, Proc. Roy. Soc. (London) Ser. A, Vol. 198, pp. 174-190 (1949)
~~6.~~7. Fey, U., M. König, and H. Eckelmann. A new Strouhal–Reynolds-number relationship for the circular cylinder in the range $47 < \mathrm{Re} < 2 \times 10^5$. Physics of Fluids, **10**(7):1547, 1998.
~~7.~~8. Maas, H.-G., A. Grün, and D. Papantoniou. Particle Tracking in three dimensional turbulent flows - Part I: Photogrammetric determination of particle coordinates. Experiments in Fluids Vol. 15, pp. 133-146, 1993.
~~8.~~9. Malik, N., T. Dracos, and D. Papantoniou Particle Tracking in three dimensional turbulent flows - Part II: Particle tracking. Experiments in Fluids Vol. 15, pp. 279-294, 1993.
10. Tropea, C., A.L. Yarin, and J.F. Foss. Springer Handbook of Experimental Fluid Mechanics. Vol. 1. Springer Science & Business Media, 2007.
11. Monaghan, J. J., and J. B. Kajtar. Leonardo da Vinci's turbulent tank in two dimensions. European Journal of Mechanics-B/Fluids. 44:1-9, 2014.
~~9.~~12. ~~White, F. M. Fluid Mechanics, 7th ed., McGraw-Hill, 2009.~~
~~10.~~13. ~~Adrian, Ronald J., and Jerry Westerweel. Particle Image Velocimetry. Cambridge University Press, 2011.~~
~~11.~~14. ~~Maas, H.-G., A. Grün, and D. Papantoniou. Particle Tracking in three dimensional turbulent flows - Part I: Photogrammetric determination of particle coordinates. Experiments in Fluids Vol. 15, pp. 133-146, 1993.~~

Formatted: Font: +Body (Cambria)

12.15. Malik, N., T. Dracos, and D. Papantoniou. Particle Tracking in three dimensional turbulent flows – Part II: Particle tracking. Experiments in Fluids Vol. 15, pp. 279-294, 1993.

Tropea, CameronC., Alexander A.L. Yarin, and John J.F. Foss. Springer Handbook of Experimental Fluid Mechanics. Vol. 1. Springer Science & Business Media, 2007.

16. Gerrard, J. H., The wakes of cylindrical bluff bodies at low Reynolds number, Phil. Trans. Roy. Soc. (London) Ser. A, Vol. 288, No. 1354, pp. 351-382 (1978)

17. Coutanceau, M. and Bouard, R., Experimental determination of the viscous flow in the wake of a circular cylinder in uniform translation. Part 1. Steady flow, J. Fluid Mech., Vol. 79, Part 2, pp. 231-256 (1977)

13.18. Kovásznay, L. S. G., Hot wire investigation of the wake behind cylinders at low Reynolds numbers, Proc. Roy. Soc. (London) Ser. A, Vol. 198, pp. 174-190 (1949)

14.19. Fey, U., M. König, and H. Eckelmann. A new Strouhal–Reynolds-number relationship for the circular cylinder in the range $47 < Re < 2 \times 10^5$, Physics of Fluids, **10**(7):1547, 1998.

15.20. Becker, H.A. Dimensionless parameters: theory and methodology. Wiley, 1976.

Formatted: Font color: Black

Formatted: Font: +Body (Cambria)

Formatted: Font: +Body (Cambria)

Figure 1

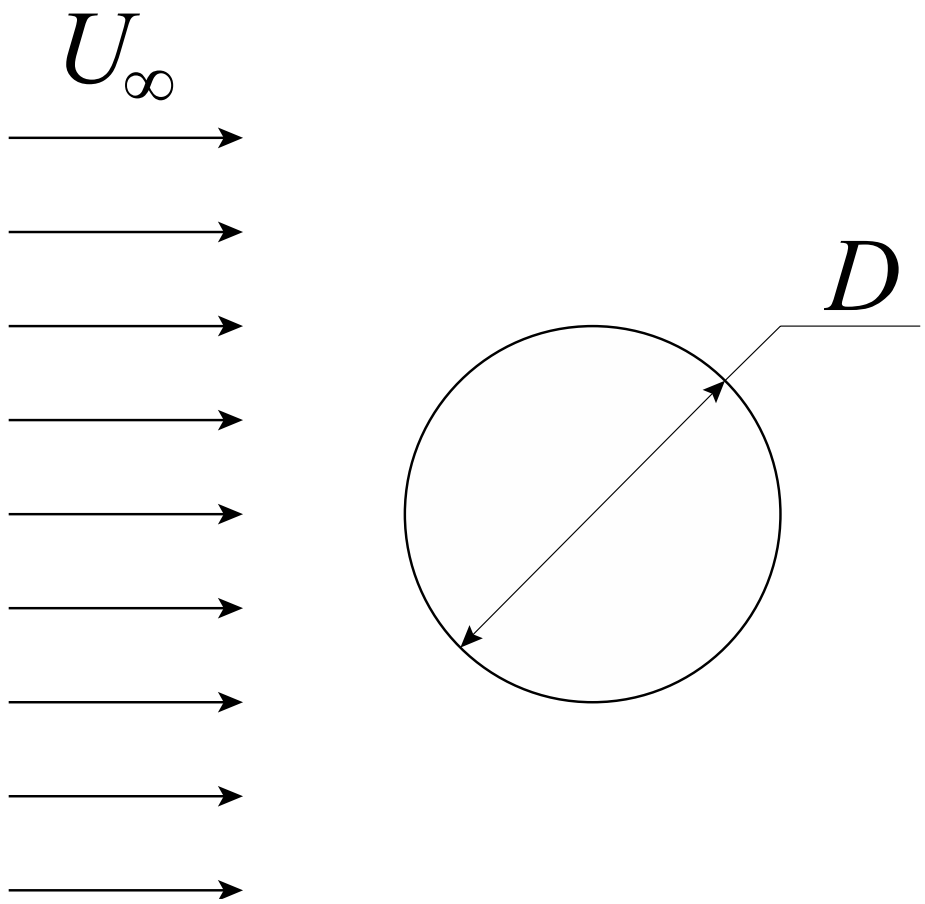

Figure 2

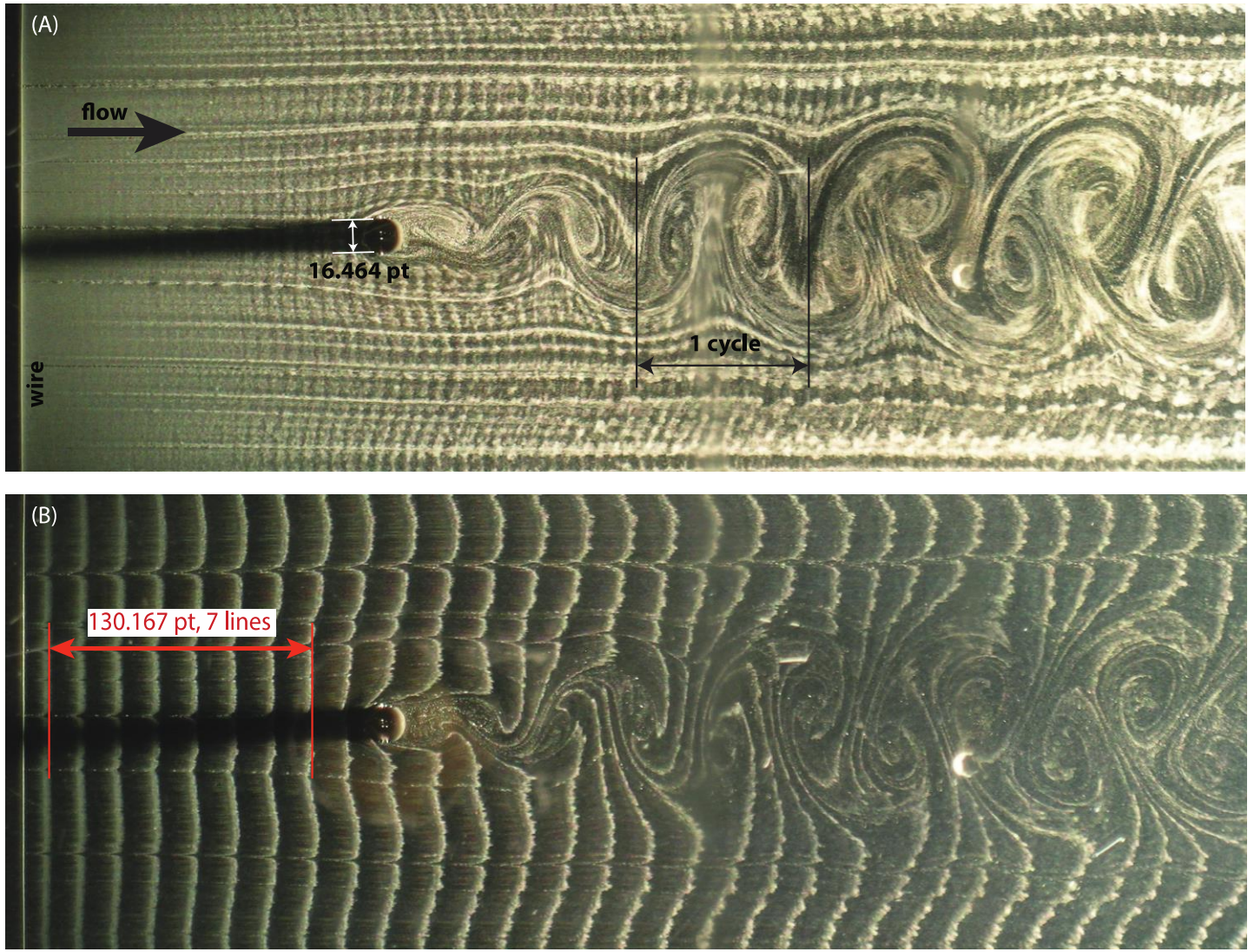

Figure 3

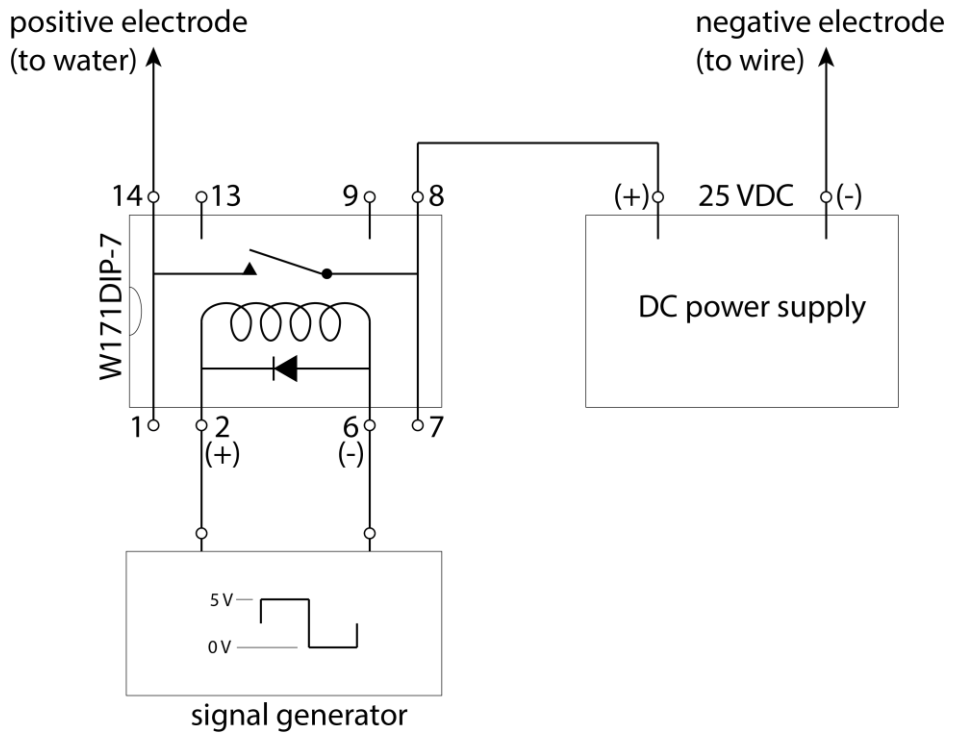
positive electrode
(to water)
negative electrode
(to wire)
14
13
9
8
(+)
25 VDC
(-)
W171DIP-7
DC power supply
1
2
6
7
(+)
(-)
5 V
0 V
signal generator

Figure 4

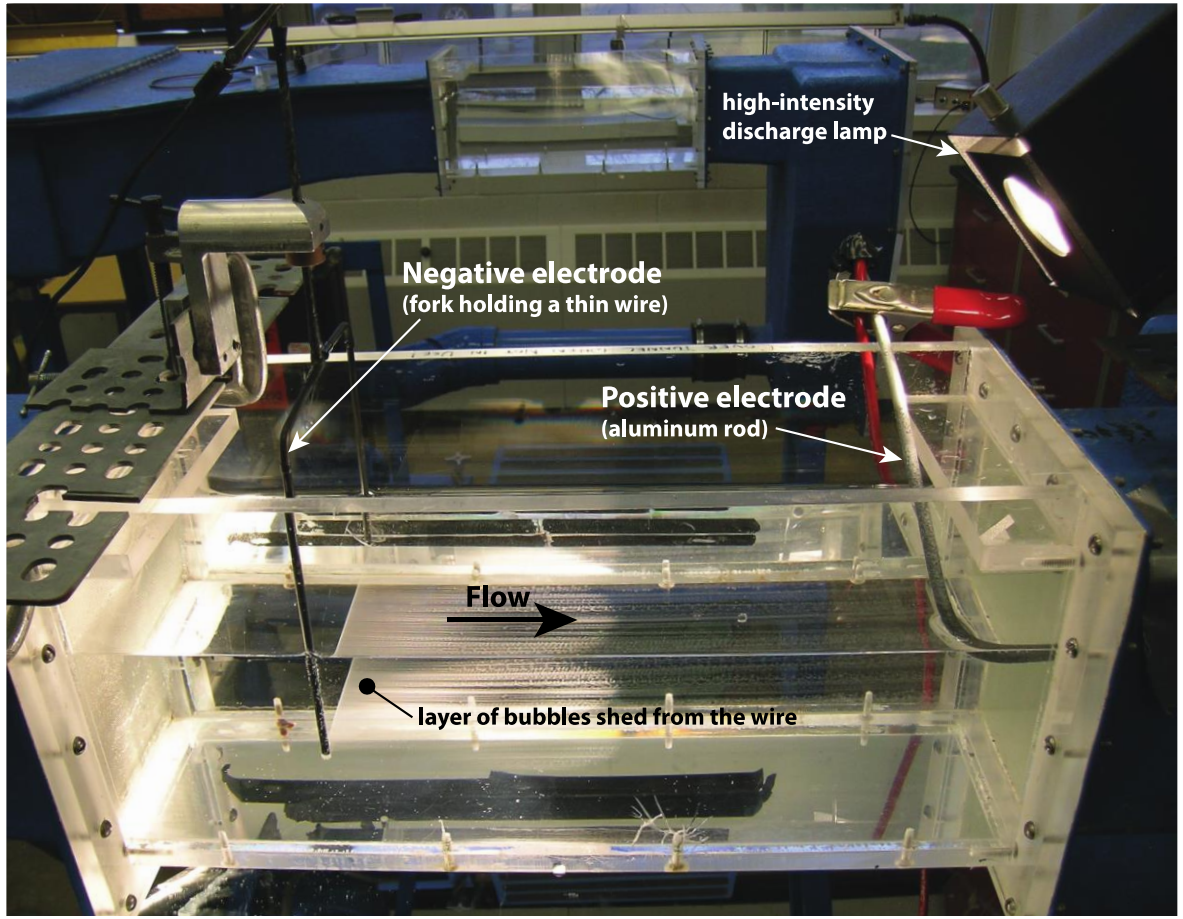
high-intensity
discharge lamp
Negative electrode
(fork holding a thin wire)
Positive electrode
(aluminum rod)
Flow
layer of bubbles shed from the wire

Figure 5

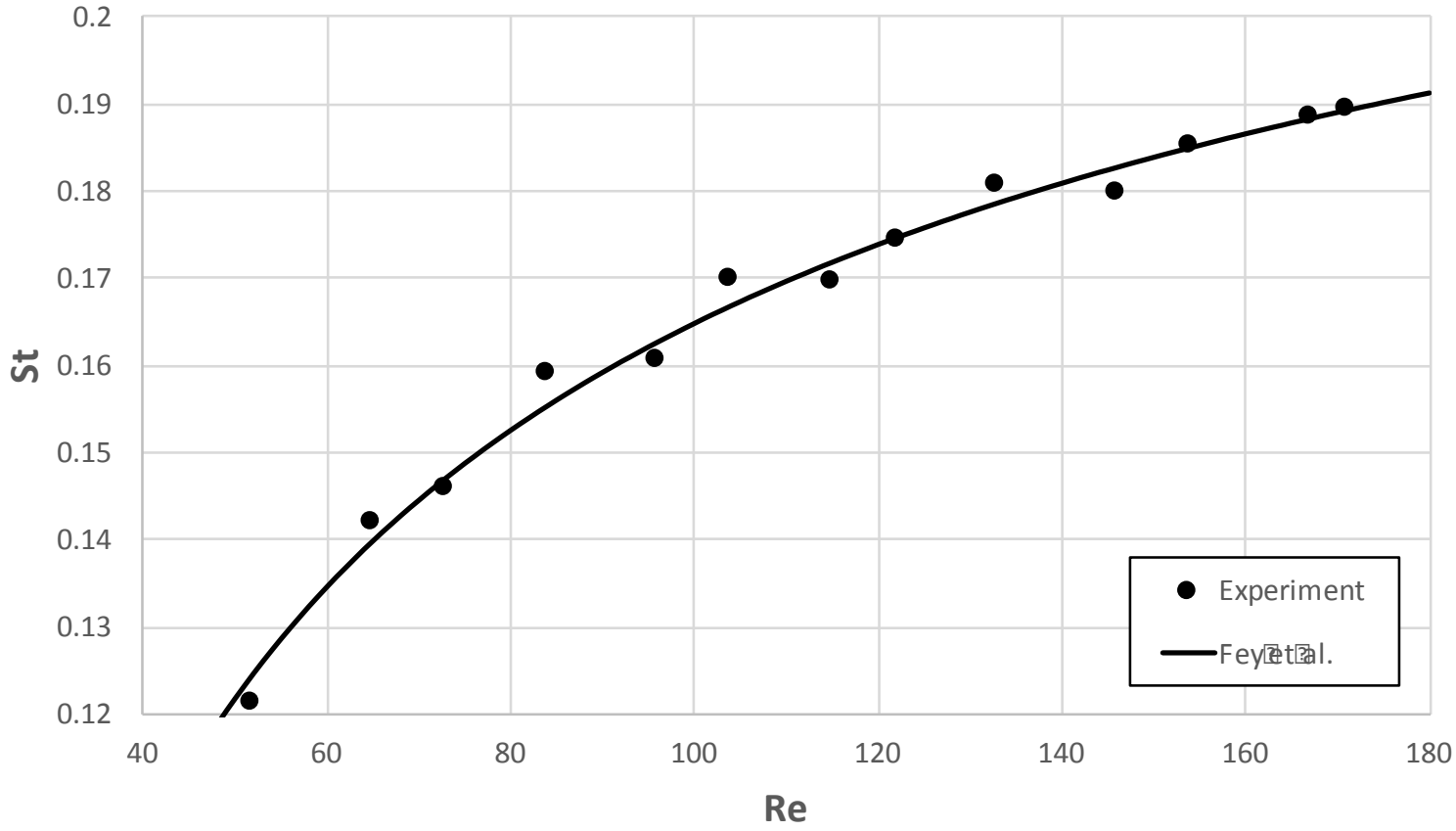
0.2
0.19
0.18
0.17
0.16
0.15
0.14
0.13
0.12
St
40
60
80
100
120
140
160
180
Re
Experiment
Fey et al.

Table 1

Re range	St*	m	Characteristic regime
$47 < \mathrm{Re} < 180$	0.2684	-1.0356	Laminar parallel shedding
$180 < \mathrm{Re} < 230$	0.2437	-0.8607	Wake transition: vortex adhesion-, A- and B-mode instability
$230 < \mathrm{Re} < 240$	0.4291	-3.6735	
$240 < \mathrm{Re} < 360$	Depends on boundary conditions		
$360 < \mathrm{Re} < 1{,}300$	0.2257	-0.4402	B-mode shedding
$1{,}300 < \mathrm{Re} < 5{,}000$	0.2040	+0.3364	KH[1]-instability in shear layer
$5{,}000 < \mathrm{Re} < 2\times10^5$	0.1776	+2.2023	Subcritical regime

[1] KH: Kelvin – Helmholtz instability

Table 2

Parameter	Value
D_{o}	0.003 m
D_{i}	14.528 pts
f_s	2.169 Hz
f_{tl}	10 Hz
L	130.167 pts
M	4842.67 pts/m
N_s	60
N_{tl}	7
T	27.66 s
U_∞	0.0384 m/s
ν	1.004×10^{-6} m²/s
Re	115
St	0.169